Antibacterial Effects of Zinc and Copper Oxide Nanoparticles and their Miscibility simulations with Polylactic acid

Dibli B. Otieno
University of Nairobi
Geoffrey O. Bosire
gbosire@uonbi.ac.ke

University of Nairobi
John M. Onyari
University of Nairobi
Julius M. Mwabora
University of Nairobi

Research Article

Keywords: Antimicrobia, effects, Chemisorption, Miscibility, Polylacti, acid, Zin, oxid, nanoparticles, Coppe, oxid, nanoparticles

Posted Date: March 27th, 2024

DOI: https://doi.org/10.21203/rs.3.rs-4150189/v1

Additional Declarations: No competing interests reported.

Antibacterial Effects of Zinc and Copper Oxide Nanoparticles and their Miscibility simulations with Polylactic acid

Dibli B. Otieno [a], Geoffrey O. Bosire [a, *], John M. Onyari [a], Julius Mwabora [b]

[a] Department of Chemistry, Faculty of Science and Technology, University of Nairobi, P.O Box 30197-00100, Nairobi

[b] Department of Physics, Faculty of Science and Technology, University of Nairobi, P.O Box 30197-00100, Nairobi

*Corresponding author: gbosire@uonbi.ac.ke/orinajeff@gmail.com

Abstract

A two-fold semi-empirical approach is reported in this study. Zinc and copper oxide nanoparticles (ZnO-NPs and CuO-NPs) were synthesized and their antibacterial effects studied. The structural properties, miscibility and adsorption behavior of ZnO and CuO nanoparticles on polylactic acid (PLA) were studied using Materials-Studio-based *ab initio* computations and density functional theory (DFT) approaches. The experimental part revealed a peak absorption at 705.95 and 525 cm^{-1} on using FTIR analysis which signified presence of spherical and rod-shaped nanoparticles for ZnO-NPs and CuO-NPs, respectively. The experimental studies affirmed that the synthesized ZnO and CuO nanoparticles exhibited antimicrobial effects on gram positive *E-coli* and gram-negative *Bacillus thuringiensis*. Theoretical investigations of pristine polylactic acid (PLA), ZnO-NPs on PLA (PLA-ZnO) and CuO-NPs on PLA (PLA-CuO) were achieved by the adsorption locator and blend modules in the Material Studio (MS) software. Both the geometrically optimized adsorbates (ZnO-NPs and CuO-NPs) were annealed on the adsorbent surface (PLA 1,1,0) to reduce the number of defects on the lattice surface. The distribution energies, phase diagrams, free energies and mixing energies revealed immiscibility of PLA/ZnO-NPs and PLA/CuO-NPs blends as evidenced by the asymmetric distribution, composition of both blends below the critical points, positive values of free energies (0.0085, 2.6871 kcal/mol) at 375K and mixing energies (0.1918,12.221 kcal/mol) respectively. In addition, the incorporation of ZnO- and CuO-NPs on the PLA polymer to control bacterial adhesion and prevent biofilm formation was also studied theoretically. The adsorption energies of ZnO and CuO NPs on the PLA surfaces were computed

and exhibited negative adsorption energies, which indicated that the type adsorption was chemisorption.

Keywords Antimicrobial effects. Chemisorption. Miscibility. Polylactic acid. Zinc oxide nanoparticles. Copper oxide nanoparticles

Introduction

New sustainable end-user cutting edge technologies, over an entire spectrum of biodegradable polymers and composites has attracted unparalleled interest the world-over. In the context of their precursors, production processes and applications, the use of nano-additives to improve specific qualities or properties.

Polylactic acid (PLA) is an interesting biodegradable thermoplastic polymer widely applied in industry [1]. For a common fact, it breaks down into constituents that are easily transformed into metabolic pathways without causing harm to the environment [2]. In addition, the application of composite materials made from polylactic acid has been on the rise in various sectors including packaging, horticulture, agriculture, household and medical field. This can be attributed to its unique properties and its ability to allow surface modification hence resulting to improved surface characteristics. There are concerted efforts in many aspects of PLA polymer design and improvements, to include additives, especially nanomaterials that possess antibacterial properties. In the same way that the development of PLA-based polymer products has revolutionized environmental protection in the context of biodegradability, the incorporation of nanomaterials in polymeric filaments prior to processing through 3D printing, has a potential of production of customized self-disinfecting objects. Reported literature has not inherently addressed surface modifications on PLA using nanomaterials, which is a nanotechnological paradigm shift in the 21st century

Being a promising aliphatic polyester, PLA exhibit high tensile strength and young's modulus, low shrinkage reducing chances of product deformation, excellent optical properties, highly biocompatibility and complete biodegradation [3–6]. Despite its notable properties, it has also been reported to be a brittle polymer, low impact strength, poor heat stability and Charpy impact fracture of about 2.5 kJ/m^2 [2, 3]. To improve on some of these properties, numerous modification methods such as annealing, physical and chemical treatments to introduce cross-linkages to the PLA

polymer, addition of nanoparticles, fibers and nucleating agents is normally done to enhance the desired properties. Equally, magnesium, silver, silicon, steel, iron and boron nitrile are added at nano- and macro-scale to enhance various purposes such as conduction, degradation, magnetic and antimicrobial properties [7–11].

Inclusion of engineered nanomaterials to polymeric surfaces is an approach that has widely been used in nanomedicine. As reported by Kim *et al* (2019) and Casalini *et al* (2019) , PLA based nanomaterials have been employed as drug delivery devices for imaging and cancer treatment [12, 13]. This is because they are able to selectively permeate through the cell to the desired affected site hence optimizing cost as well as minimizing the amount of the administered drug. Gourdon and coworkers (2017) targeted an intestinal transporter by preparing PLA-PEG nanoparticles loaded with antiviral drug (acyclovir)and functionalized with short peptides [14]. Encapsulation efficiency of adapalene was greatly improved by developing PLA-PEG and PLGA nanoparticles blended with lipid conjugate PEG, low molecular weight PCL and PLA [15]. Chiu *et al* (2008) reported on purification of MWCNT (multiwalled carbon nanotubes) using strong acids resulting to improved dispersibility and compatibility hence boosting the electrical conductivity of PLA matrix [16].

Metal oxide nanoparticles including Ag,TiO2, Zno and CuO may be added to biopolymers and synthetic polymers to impart new functionalities[17–21]. These nanomaterials not only minimize the growth of foodborne pathogens but also increase the shelf life of the packaged products [22–25].It is important to mention that United states food and drug administration (USFDA, 21CFR182.8991) acknowledges the use of zinc oxide nanoparticles as a safe additive [25, 26] .

Methods used to obtain the polymer matrix

Melt blending

This involves incorporation of nanomaterials into the molten polymer while optimizing various operation conditions. Elsewhere in literature, a melt mixer was used to melt and mix polylactic acid polymer with the nanofillers under operating conditions such as mixing speed of 50-100 rpm, temperature between 160 and 180 ^{o}C in 5 to 10 minutes [27–30]. The hot press was then used to mold the composite materials into flat sheets with controlled thickness.

In situ polymerization

As reviewed by Brezinski and Biela to polymerize lactide and CNT (carbon nanotubes), this technique involves mixing the nanofillers with the monomeric solution in presence of catalyst under the required reaction parameters to generate a polymer chain that is covalently bonded.

Solution mixing

Also known as solvent casting, this technique is categorized into three steps namely mechanical stirring of the dispersed nanoparticles in a suitable solvent, dissolving the polymer in the later dispersed solution and eradication of the solvent via lyophilization or distillation [30].Complete removal of the solvent from the polymer composite is necessary to avoid plasticization as suggested by Pinto and coworkers [31].The molten polymer matrix is then cast into a given mold to obtain the required object. The solubility of polylactic acid is effective in organic solvents such as chloroform, tetrahydrofuran (DHF), dimethylformamide (DMF), dioxane and benzene. However, it is highly insoluble in ethanol, aliphatic hydrocarbons and methanol [30, 32].

The development of devices and items through design, fabrication, prototyping and fabrication can be done using 3-dimensional printing also known as additive manufacturing. This novel technology involves a layer-by-layer processing method guided by computer aided design. Ligon *et al* reported the use of various materials for 3D printing, among them polylactic acid [33].

The daily consumption of freshly made juices and other drinks with shorter shelf lives due to consumer interest in health and good nutrition has resulted to a vast change in lifestyle. In order to maintain the desirable flavors and bioactive compounds of the packaged products, preservation is key to maintain the microbial purity and extend the shelf lives of the products. This can be achieved by incorporation of the ZnO and CuO nanoparticles to PLA bottle caps. The nanoparticles not only act as antimicrobial agents but also UV resistant hence reduces the generation of free radicals which may result to oxidative stress in the human body. This study aims at theoretically and experimentally analyzing the possibility and impact of polylactic acid polymer and nanoparticles blends. It will also help determine the effectiveness of zinc oxide and copper oxide nanoparticles against the selected gram positive and negative bacteria. Production of PLA packaging products with a self-cleaning property will reduce cases of cross contamination besides solve the threat of plastic pollution in our environment.

Materials and methods

Reagents and instruments

The following analytical grade reagents were used as received without further purification; zinc acetate dihydrate (Zn $(CH_3COO)_2{\cdot}2H_2O$), copper sulfate pentahydrate ($CuSO_4{\cdot}5H_2O$), ethanol (CH_2COOH), sodium hydroxide (NaOH) of 99% purity. Stock solutions of each salt were prepared by dissolution in distilled water.

Synthesis of zinc oxide nanoparticles

A sol gel method reported by Alwan and co-workers (2015) [34] was used to synthesize zinc oxide nanoparticles. About 8.8 g of zinc acetate dihydrate (Zn $(CH_3COO)_2{\cdot}2H_2O$) was dissolved in 100 ml distilled water to form a solution. Then, 0.1M NaOH was prepared by dissolving 4.0 g of sodium hydroxide pellets in 100 ml distilled water. The two solutions were mixed and constantly stirred at 60 $^{\circ}$C for three hours. 100 ml of ethanol was then titrated dropwise to the solution containing both zinc acetate dihydrate and sodium hydroxide until formation of a white precipitate was observed. It was left overnight to settle and later washed with distilled water to remove residual impurities and atmospheric-dried at 100 $^{\circ}$C for 4 hours. A white powder was obtained as a final product. It was then characterized using FTIR.

Synthesis of copper oxide nanoparticles

According to Rangel and co-workers [35], 0.1 M copper oxide solution was prepared by dissolving 4 g of copper sulphate in 100 ml distilled water and later stirred using a magnetic stirrer while being maintained at lower temperatures of about 50 $^{\circ}$C. Using a volume ratio of 1:1, sodium hydroxide solution was added dropwise. The solution gradually changed colour from blue to black precipitate. The black precipitate was then filtered and washed using deionized water to remove the impurities. The powder was vacuum dried for 6 hours at 80 $^{\circ}$C. The sample was then characterized using FTIR.

Antimicrobial activity of zinc oxide and copper oxide nanoparticles

Both gram positive (*Bacillus thuringiensis*) and gram negative (*Escherichia coli)* bacteria were tested to determine antimicrobial properties of the synthesized nanoparticles using well diffusion method. The two bacteria were cultured in a nutrient broth at 37 $^{\circ}$C. 100 µl culture broth having 10^6 cfv/ml of each test organism was spread on solid Muller Hinton agar plates. The plates were allowed to stand for 1 hour to allow for culture absorption. About 20 µl of the synthesized ZnO

and CuO nanoparticles solutions sample were then poured into the diffusion wells after incubation for 12 hours. The size of the zones of inhibition was later measured using an automated image processing method.

Computational Methods

Blending of PLA with zinc oxide or copper oxide nanoparticles

In this study, different PLA-nanoparticle formulations were used to determine optimal properties including compatibility, adhesion, miscibility and mixing. The Materials Studio blends module was used to predict the miscibility of polylactic acid, zinc oxide and copper oxide nanoparticles. This method shortens the discovery process and also predicts the thermodynamics of mixing the two components directly by combining the Flory-Huggins model and the molecular simulations. The derived Gibbs free energy of the mix in a binary system is described by equation 1 [36].

$$\frac{\Delta G_{mix}}{RT} = \frac{\emptyset_a}{n_a}\ln\emptyset_a + \frac{\emptyset_b}{n_b}\ln\emptyset_b + x\emptyset_a\emptyset_b \qquad (1)$$

Where $\Delta G_{mix}$is the energy for free mixing per mole, $\emptyset_b$ are volume fractions, n_a and n_b are degree of polymerization, T is the absolute temperature, R is the gas constant and the interaction parameter x. The combinatorial entropy (first two terms in equation 1) favors miscibility if it presents a negative value while the free energy due to interactions of the two components (last term) would predict immiscibility if it gives a positive value. The interaction parameter can be expressed as shown in equation 2 [36, 37].

$$x = \frac{E_{mix}}{RT} \qquad (2)$$

Here E_{mix} is the mixing energy which is the difference in interaction energies between the mixed and pure state of the components.

Since each component occupies a lattice site in the Flory-Huggins model. The mixing energy for a component with coordination number Z is shown in equation 3. The binding energy can then be defined as the interaction energies between the two components. Each component could be assigned a screen or base role. For instance, this study designated lactic acid the base role while both the nanoparticles (zinc oxide and copper oxide) were assigned screen roles.

$$\mathbf{E_{mix}} = \frac{\mathbf{1}}{\mathbf{2}}\mathbf{Z}(_{(\mathbf{E_{sb}+E_{bs}-E_{bb}-E_{ss}})}) \quad (3)$$

Whereby E_{sb} denotes binding energy of the screen-base pair (ZnO/CuO-Lactic acid), E_{bs} is the binding energy of the base-screen pair (Lactic acid-ZnO/CuO), E_{bb} signifies the binding energy of the base-base pair (Lactic acid-Lactic acid), E_{ss} represents the binding energy of the screen-screen pair (ZnO-ZnO/ CuO-CuO).

The average binding energy between the components is calculated by the excluded-volume constraint method [36]which in turn generates relative orientations of the molecules. Probability distribution function (E_{ij}) is generated by calculating pairwise interactions. Averaging the binding energies using the Boltzmann method creates a temperature dependence of the E_{ij} as expressed in equation 4 [38, 39].

$$\left(E_{ij}\right)T = \frac{\int dE_{ij} P\left(E_{ij}\right) E_{ij} \exp^{-E_{ij}/kT}}{\int dE_{ij} P\left(E_{ij}\right) e^{-E_{ij}/kT}} \quad (4)$$

It is noteworthy to mention that several factors such as chain packing, degree of crystallinity, chain flexibility, temperature, chemical nature of the individual components govern mixing for polymers. Using MS simulations, PLA and the nanoparticles were optimized using the forcite module by adopting charge using Q Eq and dreiding forcefield. The miscibility of the polylactic acid and nanoparticles was achieved using the atom base summation method in blend module.

Adsorption of ZnO and CuO nanoparticles on PLA.

Adsorption of ZnO and CuO NPs was achieved using the adsorption locator and DMol3 modules in material studio software (2021). The adsorbates (ZnO-NPs and CuO-NPs) were loaded to the adsorbent (polylactic acid) using the adsorption locator which allows configurations by carrying out Monte-Carlo simulations. Electrostatic interaction between the sorbate molecules and the framework is achieved using the Ewald &group summation method. To determine total, adsorption and deformation energies of the complex, density functional theory calculations were employed using adsorption locator module. Both adsorbates (ZnO and CuO NPs) were annealed on the adsorbent surface (PLA 1,1,0) to reduce the number of defects on the lattice surface. Optimization of the crystal model was done to adjust the structure by carrying out numerous iterations needed to converge to the minimum since directly simulating sketches molecules requires high energy

configurations which may in turn result to erroneous results. This process therefore ensured similarity to the real molecular structure.

Results and Discussion

Synthesis of ZnO-NPs and CuO-NPs

Zinc oxide nanoparticles were obtained by complete hydrolysis and condensation of zinc acetate and sodium hydroxide in an ethanol medium. Maintaining the temperature at 60 $^{\circ}$C, zinc acetate was hydrolysed into zinc and acetate ions. Zinc cations then bonded with the oxygen anions extracted from the hydroxyl group in the ethanol medium to form zinc oxide nanoparticles. This was affirmed by the presence of a white precipitate. The precipitate settled overnight and was later washed with distilled water to remove residual impurities and atmospheric-dried at 100 $^{\circ}$C for 4 hours to obtain the white zinc oxide nanoparticles (Fig. 1a). The chemical reaction of the nanoparticles synthesis is expressed as shown in equation 5.

$$Zn\,(CH_3COO)_2.2H_2O + 2NaOH \longrightarrow ZnO + 2NaCH_3COO + H_2O \qquad (5)$$

Chemical co-precipitation technique was used to synthesize copper oxide nanoparticles. Copper ions were reduced to metallic copper and later allowed to bond with oxygen to form copper oxide nanoparticles. This was evident from the systematic change of color from blue to black precipitate in Fig. 1b. The black precipitate was then filtered, washed using deionized water and dried at 80 $^{\circ}$C to obtain black copper oxide nanoparticles.

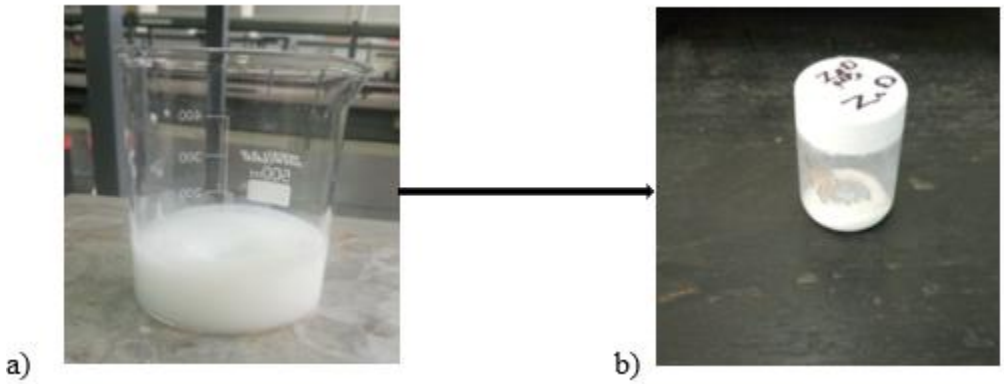

Fig. 1a Reaction stages of zinc oxide nanoparticles ((a) white precipitate b) zinc oxide nanoparticles))

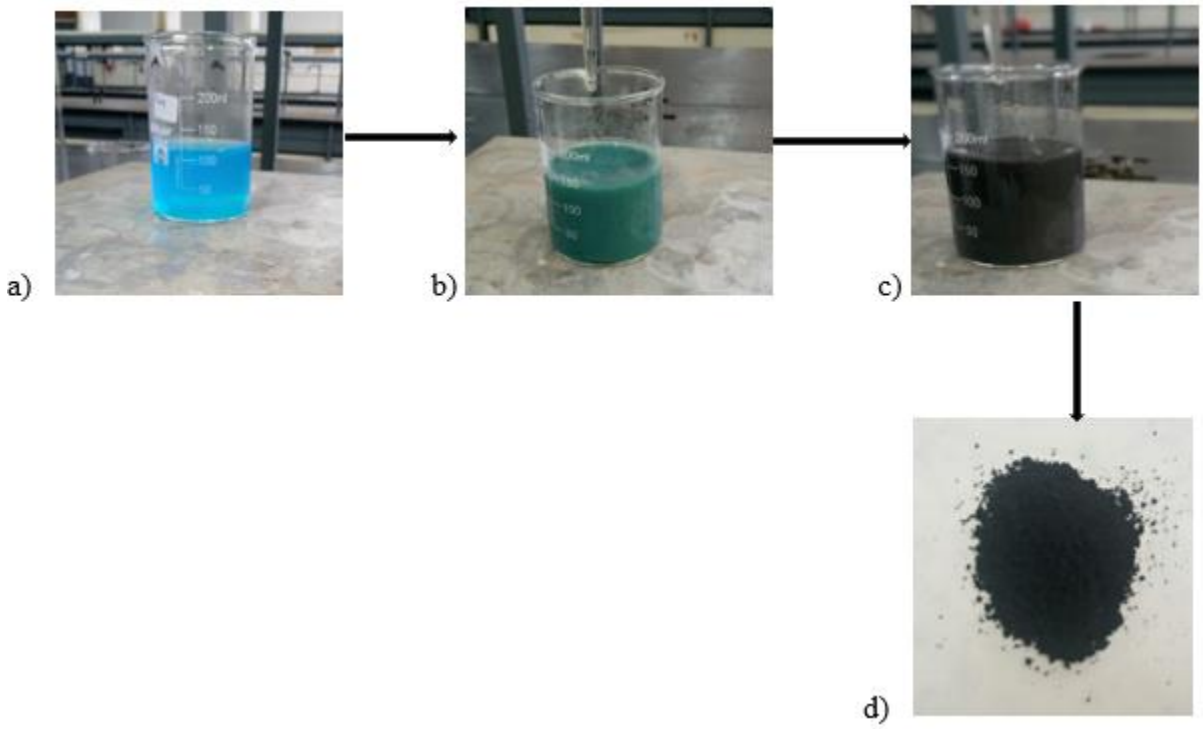

Fig. 1b Reaction stages of copper oxide nanoparticles. ((a) blue copper sulphate solution b) green precipitate c) black copper oxide precipitate d) copper oxide nanoparticles))

The synthesized zinc oxide nanocrystals had absorption peaks in the range of 705.95cm^{-1} ,829.39 cm^{-1},1047.35cm^{-1}, 1392.61cm^{-1}, 1500.62cm^{-1} and 3309.85 cm^{-1}. The presence of Zn-O bond exhibited the formation of zinc oxide compound after the annealing process which was later supported by stretching vibrations at 705.95 cm^{-1}. The absorption band at 1047.35 cm^{-1} was ascribed to C-O bond of the ethanol. The peak at 1392.61 cm^{-1} revealed the presence of a secondary alcohol. The absorption peak at 1500.62 cm^{-1} was ascribed to the stretching vibration of the alkyl group from zinc acetate while the broad absorption peak at 3309.85 cm^{-1} was ascribed to hydroxyl from ethanol. The FTIR spectrum of CuO-NPs shown in fig. 2 indicated the presence of Cu-O bond shows the formation of copper oxide compound after the annealing process which is equally attributed to Cu-O stretching modes observed at 525 and 584 cm^{-1}. The absorption peaks within the range of 1380-1640 cm^{-1} were assigned to O-H vibrations combined with copper atoms.

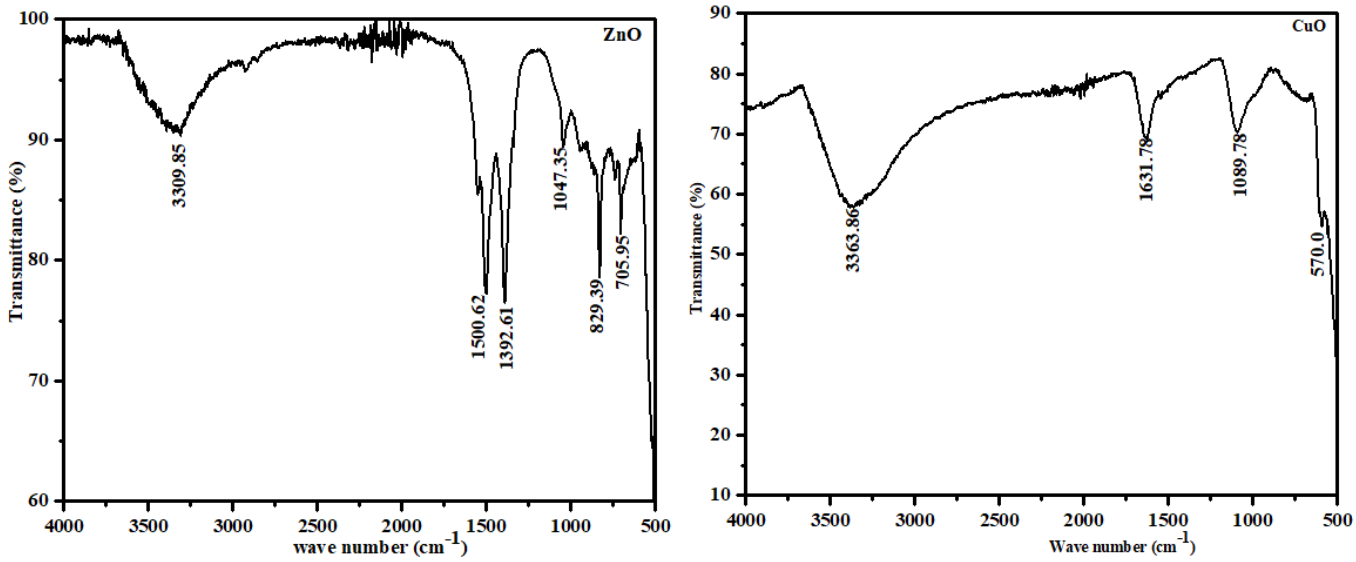

Fig. 2 FTIR spectrum for synthesized zinc oxide and copper oxide nanoparticles.

Antimicrobial activity of ZnO-NPs and CuO-NPs

Antimicrobial activity of zinc oxide and CuO nanoparticles was achieved by adopting the agar well diffusion technique using *Bacillus thuringiensis* and *Escherichia coli* as the bacterial medium. Various mechanisms including deposition of the nanoparticles on the bacteria surface, disruption of the cellular operations of the bacteria by accumulation of the NPs in the periplasmic region of the cell and formation of active hydroxyls explains the interaction of the nanoparticles and the gram positive and negative bacteria. Zinc oxide and copper oxide in particular, destroyed the cytoplasmic membrane by neutralizing the respiratory enzymes and immersing the cytoplasm contents in an outward direction. This process interfered with the cellular membrane hence killing the bacteria resulting in a zone of inhibition of bacterial growth [40, 41]. The ZnO and CuO nanoparticles generated zones of inhibition as observed in Fig. 3a and 3b. The measurements of the inhibition zones of bacterial growth have been tabulated in table 1. It is worth mentioning that in this particular study, ZnO and CuO nanoparticles had antimicrobial effect against *Escherichia coli*. Zinc oxide nanoparticles were observed to be slightly ineffective on *Bacillus thuringiensis.* Narayan and team also determined the efficacy of zinc oxide nanoparticles against *Escherichia coli* to be higher [42]. However, in a study done by Ahmed and coworkers in 2014,copper oxide nanoparticles were found to exhibit inhibitory effect against most gram negative and positive

bacterial strains including *Pseudomonas aeruginosa* and *Escherichia coli* respectively [43]. These results were equally supported by studies published elsewhere in literature [44, 45].

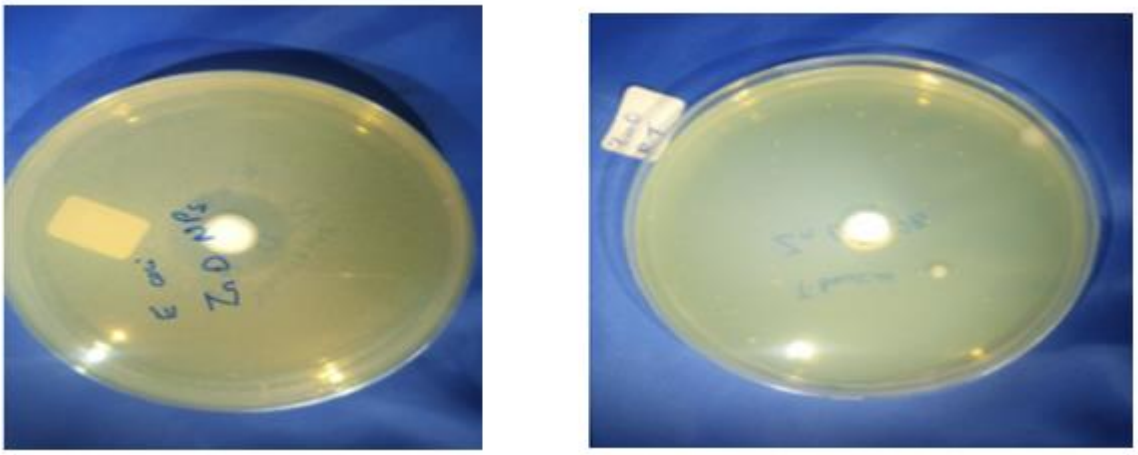

Fig. 3a Inhibition zones of zinc oxide nanoparticles on a) *Escherichia coli* b) *Bacillus thuringiensis*

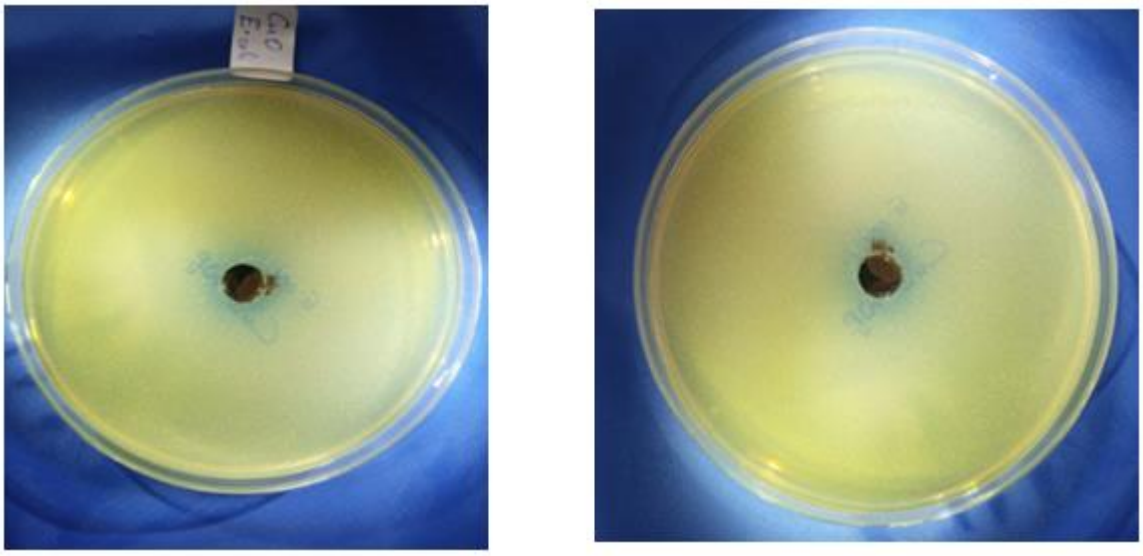

Fig. 3b Inhibition zones of copper oxide nanoparticles on a) *Escherichia coli* b) *Bacillus thuringiensis*

Table 1 Inhibition measurements of zinc oxide and copper oxide nanoparticles

Sample	Bacteria	Scientific name	Bacteria type	Inhibition zone (mm)

ZnO NPs	E. coli	*Escherichia coli*	Gram negative	371.96
CuO NPs	E. coli	*Escherichia coli*	Gram negative	170.47
ZnO NPs	B.t	*Bacillus thuringiensis*	Gram positive	N/A
CuO-NPs	B.t	*Bacillus thuringiensis*	Gram positive	110.34

Computational Models of the geometrically optimized structures.

The optimized models were built using the material studio software 2021 user interface (Fig. 4). The lattice parameters employed in developing respective unit cells have been shown in table 2. Supercell units of 3x3x1 were created using the symmetry calculations for both the polymer and metal oxide structures and later optimized using BFGS algorithm.

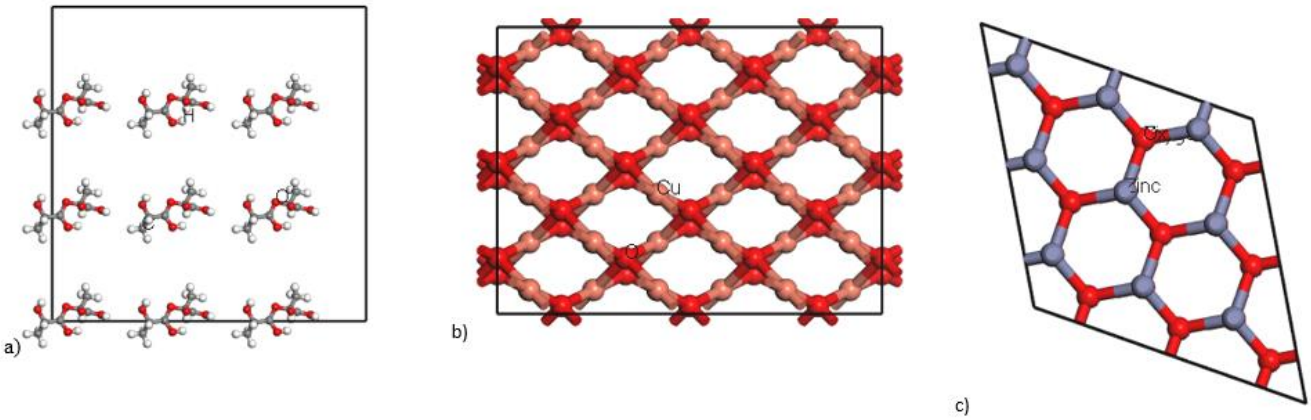

Fig. 4 Crystal models of a) PLA b) CuO c) ZnO

Table 2 lattice parameters for PLA, CuO and ZnO crystals

Structure	Lattice parameters (A)	Space group	Cell angle	Lattice type
PLA crystal	a =30.00 b =30.00 c=10.00	P1	Alpha=90.00 Beta = 90.00 Gamma=90.00	3D triclinic
CuO crystal	a=13.959 b=10.230	P1	Alpha =90.00 Beta =90.00	3D triclinic

ZnO crystal	c=5.108 a =9.7478 b =9.7478 c=5.2054	P1	Gamma=90.00 Alpha=90.00 Beta = 90.00 Gamma=90.00	3D triclinic

Blending of polylactic acid and zinc oxide and copper oxide nanoparticles

Polylactic acid and the nanoparticles were screened for compatibility. The lactic acid monomer was geometrically optimized before carrying out blend calculations. ZnO-NPs and CuO-NPs were screened against lactic acid (base role). This aided in calculations of the binding and mixing energies of the polymer and the nanoparticles. Setting up the head and tail atom on the repeat units were signified by presence of cyan and magenta cages around the respective atoms (Fig. 5). This minimized close contact with any other atom in the system hence allowing the monomer to mimic the rest of the `polymer which was represented by the non-contact atoms [38].

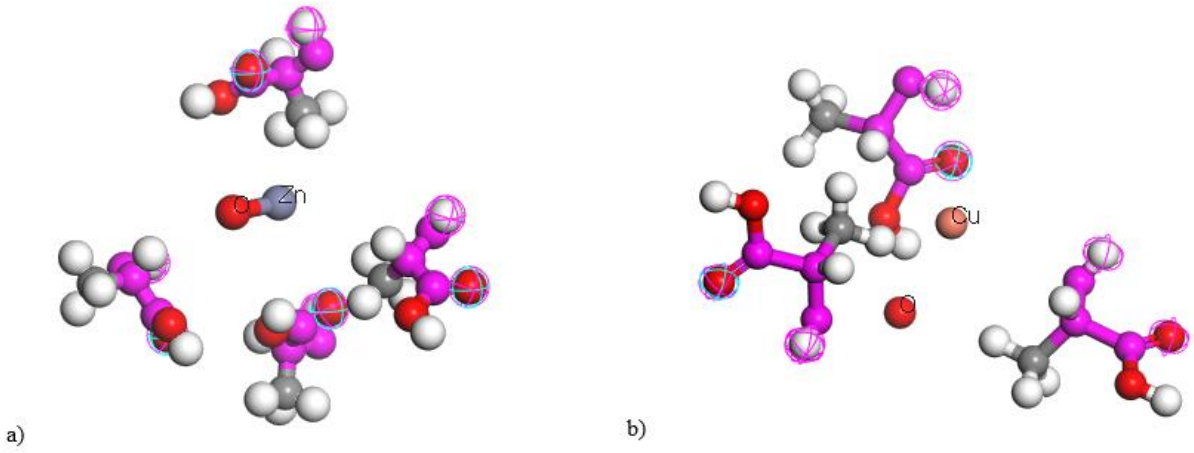

Fig. 5 PLA-ZnO and PLA-CuO blend (the cyan and magenta cages represent the head and tail atoms)

Blends binding energy distribution

According to the distribution graphs, the binding energies of the lactic-lactic (Ebb), lactic-ZnO (Ebs), ZnO-ZnO (Ess) do not have similar energy distributions hence the blend system is

immiscible. PLA-CuO energy distribution is not symmetrical therefore it forms an immiscible blend. This is equally supported by the positive chi parameter (0.3238) and the Emix (0.1918) values.

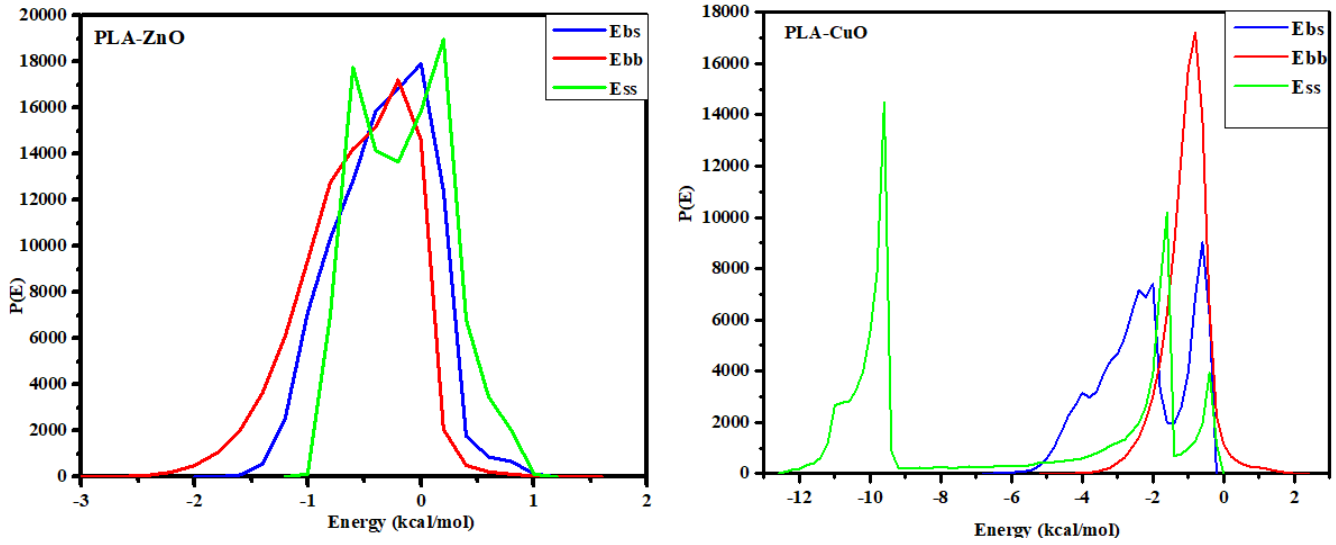

Fig. 6 Energy distribution of PLA-ZnO and PLA-CuO mixtures

Mixing energies and Flory-Huggin's interaction parameters

The interaction chi parameter and mixing energies are important factors in determining the compatibility of a binary system. The two components would prefer to mix if the chi parameter is negative. In contrast, a positive value indicates the two components are immiscible. Similarly positive mixing energies would be attributed to immiscibility while a negative mixing energy would be ascribed to the two components tending to mix together under an exothermic process [46, 47]. The immiscibility of PLA-ZnO and PLA-CuO was supported by the positive chi parameter (0.3238,20.632) and the E_{mix} (0.1918,12.221) values respectively within a temperature range of 100-500K.

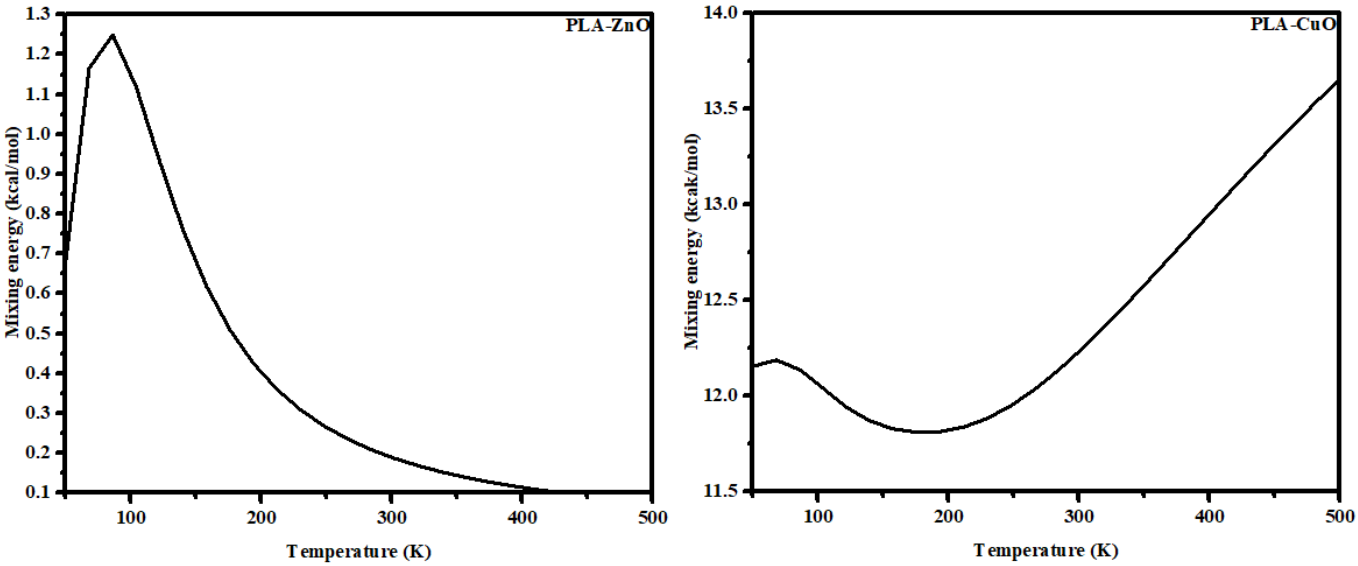

Fig. 7 Mixing energies for PLA-ZnO and PLA-CuO blends against temperature

Free energies

The free energies for each binary mixture at different temperatures and volume fractions was computed via equation 1. The blend is expected to be miscible if $\Delta G_{mix} < 0$ [36] and only one minimum point exists on the curve while immiscible if $\Delta G_{mix} > 0$.The binary systems were computed at different temperatures and polymerization degree of polylactic acid set to 10000.As observed in Fig. 8, the free energies for PLA/CuO NPs were positive at all temperatures hence revealing miscibility for the binary system. At a temperature of 500K, the free energies are negative therefore PLA/ZnO blend is slightly miscible and regarded immiscible at temperatures 50,162.5.275 and 387.5K since all the free energies were positive.

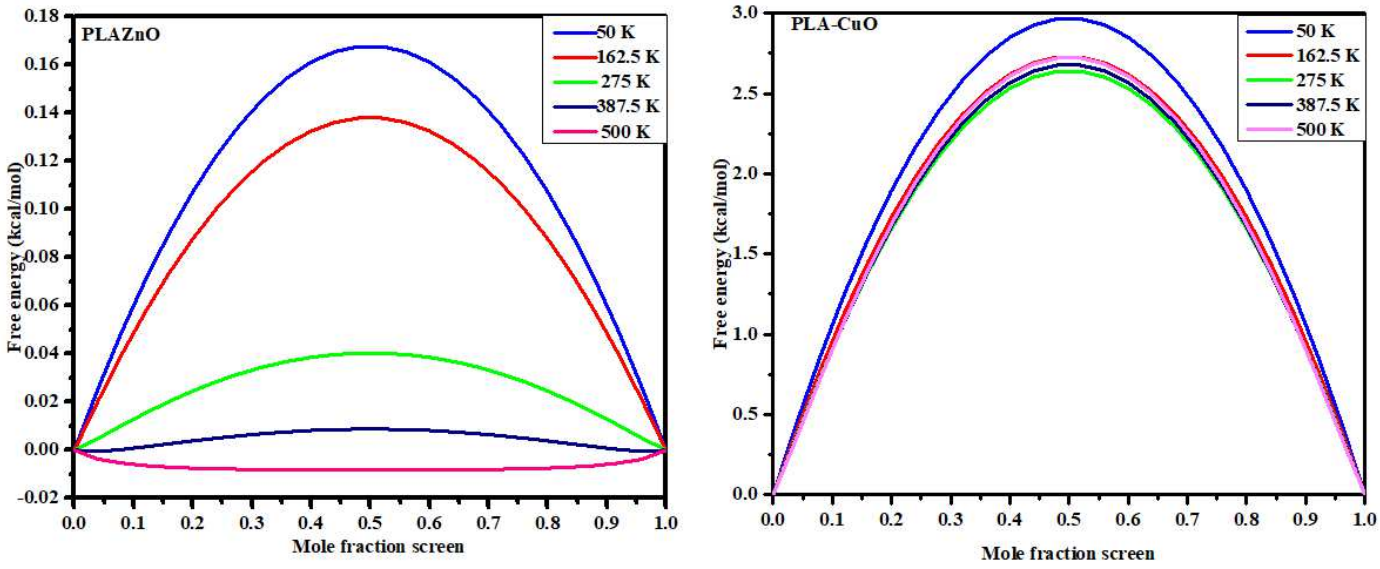

Fig. 8 Free energies of PLA-ZnO-NP and PLA-CuO-NP blend against mole fractions

Phase diagrams

Phase diagrams aid in determining the compatibility and stability of various binary mixtures. It is obtained from the derivatives of free energy ΔG_{mix} to volume fractions [48]. The spinodal and binodal curves are simulated from the second and first order derivatives of the free energy. Critical point is the intersection point of the two curves. Not all mixtures have critical points according to Flory-Huggins model, this could result to miscibility of the components at any given temperature [49]. The region outside the binodal curve is stable hence a miscible binary mixture while the region between the spinodal (green line) and binodal (blue line) curve is known to be metastable implying that the concentration variation of any phase may result to separation within the blend [36]. The unstability of the region within the spinodal curve causes spontaneous phase separation of the binary mixtures. In addition, increasing the polymerization degree decreases the rate of miscibility. The critical temperatures for PLA-ZnO and PLA-CuO blends are 495 and 3250 K respectively as shown in figure 9. The region within the spinodal curve for the PLA-ZnO and PLA-CuO blends equally support immiscibility. The results further show that both blends are miscible at temperatures above the critical points.

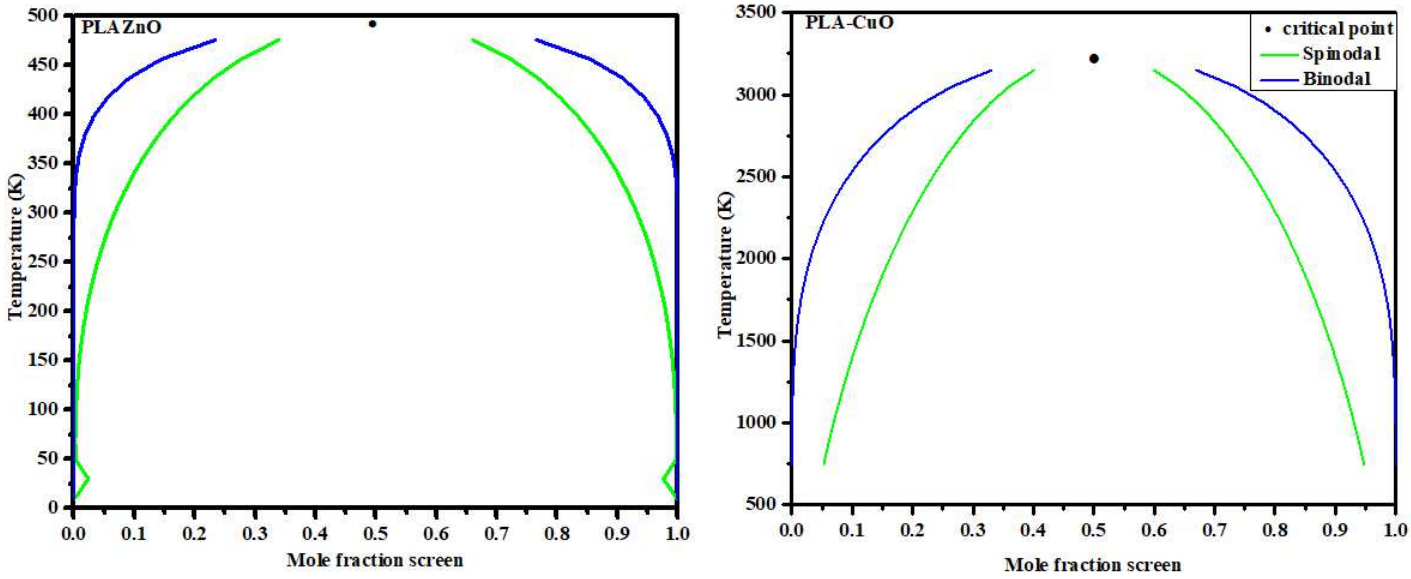

Fig. 9 Phase diagrams of PLA-ZnO and PLA-CuO blends

Adsorption of zinc oxide and copper oxide nanoparticles on PLA surface

Modification of the frequently touched surfaces PLA surface with ZnO and CuO nanoparticle makes it less susceptible to bacterial infections. This is because it is able to effectively kill microbe colony and prevent bacterial colonization [50]. Various factors such as chemical and topological characteristics influence the rate of microorganism adhesion on numerous polymer surfaces. For instance, a rougher PLA surface would provide more surface area for microbe adhesion than a smoother surface. In reference to chemical characteristics, hydrophobic surfaces are more prone to microorganisms than the hydrophilic surfaces [50–54]. A number of studies have been done on the mechanism of antimicrobial activity of nano ZnO and CuO and their dependence on size and shape [42, 43, 55]. Adsorption of ZnO and CuO NPs on PLA (1,1,0) can be simulated as shown in fig. 10. This would aid in determination of the binding, adsorption energy and prediction of the adsorption isotherm associated to this process. The cleaved surface generated vacant sites to which the ZnO and CuO nanoparticles would be later adsorbed.

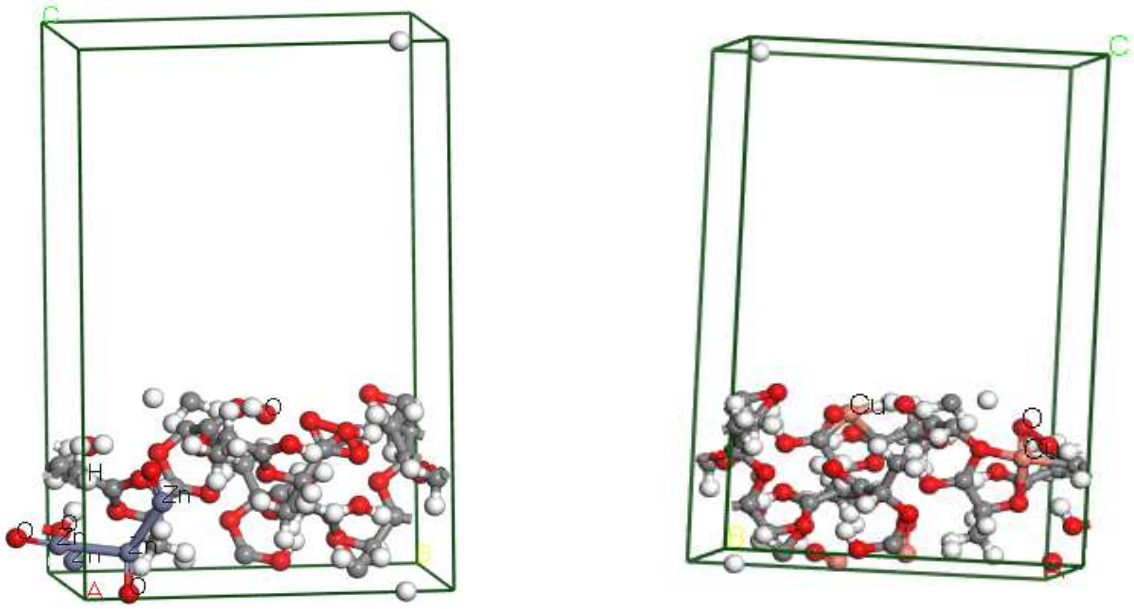

Fig. 10 Adsorbed ZnO and CuO nanoparticles on polylactic acid surface. (The red color represents oxygen atom, white shows hydrogen atom, grey signifies carbon atom, bluish grey represents zinc atom and red-orange signifies copper atom)

Incorporation of a ZnO-NPs and CuO-NPs to the polylactic acid resulted to a final adsorption energy of -92.4486 and -654.8616 kcal/mol as expressed in table 3. The antibonding and bonding state is created by assuming of being tightly localized, the adsorbate induced level is modelled as a single layer after interaction of carbon and oxygen 2P orbital with the zinc and copper 3d state. Presence of an empty antibonding state which is caused by the shift of the 3d orbital above the fermi level results to a net attractive force between the nanoparticles and the polylactic acid. Having fulfilled various characteristics of chemisorption including defined as a monolayer process, an irreversible reaction due to involvement of chemical bonding between the molecules. Energy of adsorption has been determined from the sum of deformation and rigid adsorption energy. It describes the energy, in kcal/mol, released when the unrelaxed base PLA and nanoparticles constituents are adsorbed on the PLA surface (1,1,0) while deformation energy is the energy in kcal/mol, released when the adsorbed PLA-ZnO and PLA-CuO NPS are relaxed on the PLA surface (1,1,0).

Table 3 Adsorption energy of PLA-ZnO and PLA-CuO interactions.

No of configurations	Structure	Total energy	Adsorption energy	Rigid adsorption energy	Deformation energy	ZnO;dEad/dNi
1	PLA-ZnO	-1.6285	-92.8022	-1.6285	-91.1737	-92.8022
2	PLA-ZnO	-1.6115	-92.7853	-1.6116	-91.1737	-92.7853
3	PLA-ZnO	-1.5571	-92.7309	-1.5571	-91.1737	-92.7309
4	PLA-ZnO	-1.3853	-92.5591	-1.3853	-91.1737	-92.5591
5	PLA-ZnO	-1.2748	-92.4486	-1.2748	-91.1737	-92.4486
6	PLA-CuO	-7.1914	-656.5111	-7.1915	-649.3197	-130.231
7	PLA-CuO	-6.7210	-656.0407	-6.7211	-649.3196	-130.675
8	PLA-CuO	-6.1698	-655.4895	-6.1698	-649.3196	-130.511
9	PLA-CuO	-5.8213	-655.1410	-5.8213	-649.3196	-130.708
10	PLA-CuO	-5.5419	-654.8616	-5.5419	-649.3197	-130.608

Prediction of adsorption isotherm

The theoretical results showed that adsorption of zinc oxide and copper oxide nanoparticle on polylactic polymer surface follow Langmuir equation for adsorption (equation 6) since it describes monolayer adsorption. In addition, it also gives clarity on surface homogeneity, distribution of binding sites and the energies required to facilitate bonding of the adsorbate on the adsorbent surface [56, 57].

$$\frac{C_e}{q_e} = \frac{1}{K_L q_m} + {C_e}/{q_m} \qquad (6)$$

Where $C_e$and q_e are amount of unadsorbed adsorbate concentration and adsorbed adsorbate in solution at equilibrium respectively, K_L is the Langmuir constant and q_m is the maximum adsorption capacity [58].

Conclusions

Zinc oxide and copper oxide nanoparticles were synthesized by sol gel and co-precipitation techniques respectively. zinc oxide compound was ascribed to stretching vibrations at 705.95 cm^{-1} while Cu-O stretching modes were observed at 525 and 584 cm^{-1} from the FTIR spectra. The synthesized ZnO and CuO nanoparticles exhibited antibacterial effects on gram negative

Escherichia coli and little effect on Bacillus thuringiensis. Through computational studies, strong affinity exhibited by the strong intermolecular forces between ZnO-C, ZnO-O and CuO-C bonds resulted to an interconnection between PLA and the nanoparticles hence a stronger adhesion which further ensured the antimicrobial action would be effective for a longer duration. Polylactic acid polymer was theoretically determined to be immiscible with Zinc oxide and copper oxide nanoparticles. This is evident from the positive chi parameter, free and mixing energies. Both PLA-ZnO and PLA-CuO blends were predicted to be miscible at temperatures above the critical points as observed from their respective phase diagrams. ZnO and CuO nanoparticles were adsorbed on PLA surface (1,1,0) through a chemisorption process.

Future perspectives

The novelty of additive manufacturing coupled with application of improved biodegradable polymers has been foreseen to cut on the ubiquitous plastic waste in the environment hence 3D printing of polymer blends, composites and surface coated biodegradables. Researchers are also encouraged to carry out more theoretical computations to complement the laboratory tests. Vast application of polymer blends and composites with antimicrobial properties and corresponding product tests in various fields.

Author contributions

Conceptualization was done by DO, GB, JO and JM; Investigation, methodology and formal analysis was done by DO, GB, JO and JM; Supervision was done by GB, JO and JM; Validation was done by GB, JO and JM; Visualization was done DO; Writing—original draft were done by DO; Writing—review & editing were done by DO, GB, JO and JM.

Funding

This research did not receive any specific grant from funding agencies in the public, commercial, or not-for-profit sectors.

Declarations

Conflict of interest

The authors declare that they have no known financial interests or personal relationships that could have appeared to influence the work reported in this paper

Acknowledgements

The authors would like to acknowledge Dr Elizabeth Ndunda (Machakos University) for the provision of the Material Studio Software (V.2021) and Ephraim Muriithi who offered MS training. Solomon Chogo who assisted in carrying out some of antibacterial tests of the nanoparticles.

References

1. Jem KJ, Tan B (2020) The development and challenges of poly (lactic acid) and poly (glycolic acid). *Adv Ind Eng Polym Res,* 3:60–70. https://doi.org/10.1016/j.aiepr.2020.01.002

2. Oksiuta Z, Jalbrzykowski M, Mystkowska J, Romanczuk E, Osiecki T (2020) Mechanical and Thermal Properties of Polylactide (PLA) Composites Modified with Mg, Fe, and Polyethylene (PE) Additives. *Polym* 12:2939. https://doi.org.10.3390/polym12122939

3. Domb AJ, Kumar N (2011) Biodegradable polymers in clinical use and clinical development. John Wiley & Sons

4. Żenkiewicz M, Rytlewski P, Malinowski R (2010) Compositional, physical and chemical modification of polylactide. *J Achiev Mater Manuf Eng* 43:192–199

5. Luckachan GE, Pillai CKS (2011) Biodegradable polymers-a review on recent trends and emerging perspectives. *J Polym Environ* 19:637–676. https://doi.org/10.1007/s10924-011-0317-1

6. Norazlina H, Kamal Y (2015) Graphene modifications in polylactic acid nanocomposites: a review. *Polym Bull* 72:931–961. https://doi.org/10.1007/s00289-015-1308-5

7. Cifuentes SC, Frutos E, Benavente R, Lorenzo V, González-Carrasco JL (2017) Assessment of mechanical behavior of PLA composites reinforced with Mg micro-particles through depth-sensing indentations analysis. *J Mech Behav Biomed* 65:781–790. https:// doi. org/ 10. 1016/j. jmbbm. 2016. 09. 013

8. Cifuentes SC, Gavilán R, Lieblich M, Benavente R, González-Carrasco JL (2016) In vitro degradation of biodegradable polylactic acid/magnesium composites: Relevance of Mg particle shape. *Acta biomater* 32:348–357. https://doi,org/10.1016/j.actbio.2015.12.037

9. Tan LJ, Zhu W, Zhou K (2020) Recent progress on polymer materials for additive manufacturing. *Adv Funct Mater* 30:2003062. https:// doi. org/ 10. 1002/ adfm. 20200 3062

10. Jiang D, Ning F (2020) Fused Filament Fabrication of Biodegradable PLA/316L Composite Scaffolds: Effects of Metal Particle Content. Procedia Manufacturing 48:755–762. https://doi.org/10.1016/j.promfg.2020.05.110

11. Ferri JM, Motoc DL, Bou SF, Balart R (2019) Thermal expansivity and degradation properties of PLA/HA and PLA/βTCP in vitro conditioned composites. *J Therm Anal Calorim* 138:2691–2702. https://doi.org/10.1007/s10973-019-08799-0

12. Casalini T (2017) Bioresorbability of polymers: Chemistry, mechanisms, and modeling. In: Bioresorbable Polymers for Biomedical Applications. Elsevier, pp 65–83. https://doi.org/10.1016/B978-0-08-100262-9.00003-3

13. Kim K-T, Lee J-Y, Kim D-D, Yoon IS, Cho HJ (2019) Recent progress in the development of poly (lactic-co-glycolic acid)-based nanostructures for cancer imaging and therapy. Pharmaceutics 11:280. https://doi.org/10.3390/pharmaceutics11060280

14. Gourdon B, Chemin C, Moreau A, Arnauld T, Baumy P, Cisternino S, Pean JM, Decleves X (2017) Functionalized PLA-PEG nanoparticles targeting intestinal transporter PepT1 for oral delivery of acyclovir. *Int j pharm* 529:357–370. https://doi.org/10.1016/j.ijpharm.2017.07.024

15. Medina DX, Chung EP, Bowser R, Sirianni RW (2019) Lipid and polymer blended polyester nanoparticles loaded with adapalene for activation of retinoid signaling in the CNS following intravenous administration. *J Drug Deliv Sci Technol* 52:927–933. https://doi.org/10.1016/j.jddst.2019.04.013

16. Chiu W-M, Chang Y-A, Kuo H-Y, Lin MH, Wen HC (2008) A study of carbon nanotubes/biodegradable plastic polylactic acid composites. Journal of Applied Polymer Science 108:3024–3030. https://doi.org/10.1002/app.27796

17. Mizielińska M, Kowalska U, Jarosz M, Sumińska P, Landercy N, Duquesne E (2018) The Effect of UV Aging on Antimicrobial and Mechanical Properties of PLA Films with Incorporated Zinc Oxide Nanoparticles. *Int J Environ Res Public Health* 15:794. https://doi.org/10.3390/ijerph15040794

18. Silvestre C, Duraccio D, Marra A, Strongone V, Cimmino S (2016) Development of antibacterial composite films based on isotactic polypropylene and coated ZnO particles for active food packaging. Coatings 6:4. https://doi.org/10.3390/coatings6010004

19. Li W, Zhang C, Chi H, Li L, Lan T, Han P, Chen H, Qin Y (2017) Development of antimicrobial packaging film made from poly (lactic acid) incorporating titanium dioxide and silver nanoparticles. *Molecules* 22:1170. https://doi.org/10.3390/molecules22071170

20. Marvizadeh MM, Oladzadabbasabadi N, Nafchi AM, Jokar M (2017) Preparation and characterization of bionanocomposite film based on tapioca starch/bovine gelatin/nanorod zinc oxide. *Int j biol macromol* 99:1–7. https://doi.org/10.1016/j.ijbiomac.2017.02.067

21. Li W, Li L, Cao Y, Lan T, Chen H, Qin Y (2017) Effects of PLA film incorporated with ZnO nanoparticle on the quality attributes of fresh-cut apple. *Nanomaterials* 7:207. https://doi.org/10.3390/nano7080207

22. Marra A, Rollo G, Cimmino S, Silvestre C (2017) Assessment on the effects of ZnO and Coated ZnO particles on iPP and PLA properties for application in food packaging. *Coatings* 7:29. https://doi.org/10.3390/coatings7020029

23. Akbar A, Anal AK (2014) Zinc oxide nanoparticles loaded active packaging, a challenge study against Salmonella typhimurium and Staphylococcus aureus in ready-to-eat poultry meat. *Food control* 38:88–95. https://doi.org/10.1016/j.foodcont.2013.09.065

24. Mizielińska M, \Lopusiewicz \Lukasz, Mężyńska M, Bartkowiak A (2017) The influence of accelerated UV-A and Q-SUN irradiation on the antimicrobial properties of coatings

containing ZnO nanoparticles. *Molecules* 22:1556. https://doi.org/10.3390/molecules22091556

25. Bartkowiak A, Mizielińska M, Sumińska P, Romanowska-Osuch A, Lisiecki S (2016) Innovations in food packaging materials. *In: Emerging and Traditional Technologies for Safe, Healthy and Quality Food. Springer*, pp 383–412. https://doi.org/10.1007/978-3-319-24040-4_19

26. Wang Y, Ma J, Xu Q, Zhang J (2017) Fabrication of antibacterial casein-based ZnO nanocomposite for flexible coatings. *Mater Des*, 113:240–245. https://doi.org/10.1016/j.matdes.2016.09.082

27. Ali AM, Ahmad SH (2013) Mechanical characterization and morphology of polylactic acid/liquid natural rubber filled with multi walled carbon nanotubes. In: AIP conference proceedings. American Institute of Physics, pp 83–89. https://doi.org/10.1063/1.4858634

28. Chieng BW, Ibrahim NA, Wan Yunus WMZ, Hussein MZ (2013) Poly (lactic acid)/poly (ethylene glycol) polymer nanocomposites: Effects of graphene nanoplatelets. *Polym* 6:93–104. https://doi.org/10.3390/polym6010093

29. Bao C, Song L, Xing W, Yuan B, Wilkie CA, Huang J, Guo Y, Hu Y (2012) Preparation of graphene by pressurized oxidation and multiplex reduction and its polymer nanocomposites by masterbatch-based melt blending. *J Mater Chem* 22:6088–6096. https:// doi.org/ 10.1039/C2JM16203B

30. Gonçalves C, Gonçalves IC, Magalhães FD, Pinto AM (2017) Poly (lactic acid) Composites Containing Carbon-Based Nanomaterials: A Review. Polym 9:269. https://doi.org/10.3390/polym9070269

31. Pinto AM, Cabral J, Tanaka DAP, Mendes AM, Magalhães FD (2013) Effect of incorporation of graphene oxide and graphene nanoplatelets on mechanical and gas permeability properties of poly (lactic acid) films. *Polym Int* 62:33–40. https://doi.org/10.1002/pi.4290

32. Huang X, Yin Z, Wu S, Qi X, He Q, Zhang Q, Yan Q, Boey F, Zhang H (2011) Graphene-based materials: synthesis, characterization, properties, and applications. *small* 7:1876–1902. https://doi.org/10.1002/smll,201002009

33. Ligon SC, Liska R, Stampfl J, Gurr M, Mülhaupt R (2017) Polymers for 3D printing and customized additive manufacturing. *Chem Rev* 117:10212–10290. https://doi.org/10.1021/acs.chemrev.7b00074

34. Alwan RM, Kadhim QA, Sahan KM, Ali RA, Mahdi RJ, Kassim NA, Jassim AN (2015) Synthesis of zinc oxide nanoparticles via sol–gel route and their characterization. *Nanosci Nanotechnol* 5:1–6. https:// doi.org/ 10.5923/j.nn.20150501.01

35. Rangel WM, Santa RAAB, Riella HG (2020) A facile method for synthesis of nanostructured copper (II) oxide by coprecipitation. *J Mater Res Technol* 9:994–1004. https://doi.org/10.1016/j.jmrt.2019.11.039

36. Abdalla MAM, Peng H, Wu D, Abusin L, Mbah TJ (2018) Prediction of Hydrophobic Reagent for Flotation Process Using Molecular Modeling. ACS Omega 3:6483–6496. https://doi.org/10.1021/acsomega.8b00413

37. Abderaman MB, Talla K, Gueye E-HO, Dione AN, Faye O, Beye AC (2018) A Molecular Dynamics Simulation Study on the Miscibility of Polyglycolide with Polyacrylonitrile. *J Polym Biopolym Phys Chem* 6:31–38. https://doi.org/10.12691/jpbpc-6-1-4

38. Blanco M (1991) Molecular silverware. I. General solutions to excluded volume constrained problems. *J Comput Chem* 12:237–247. https:doi.org/10.1002/jcc.540120214

39. González-Álvarez MJ, Balbuena P, Mellet CO, Fernández JMG, Mendicuti F (2008) Study of the Conformational and Self-Aggregation Properties of 2I,3I-O-(o-Xylylene)-per-O-Me-α- and -β-cyclodextrins by Fluorescence and Molecular Modeling. J Phys Chem B 112:13717–13729. https://doi.org/10.1021/jp077670c

40. Chopra R, Kashyap N, Kumar A, Banerjee D (2020) Chemical Synthesis of Copper Oxide Nanoparticles Study of its Optical and Electrical Properties. *Int J Eng Res Technol* and V9:. https://doi.org/10.17577/IJERTV9IS010160

41. Sirelkhatim A, Mahmud S, Seeni A, Kaus NHM, Anne LC, Bakhori SKM, Hasan H, Mohamad D (2015) Review on Zinc Oxide Nanoparticles: Antibacterial Activity and Toxicity Mechanism. *Nanomicro Lett* 7:219–242. https://doi.org/10.1007/s40820-015-0040-x

42. Narayanan PM, Wilson WS, Abraham AT, Sevanan M (2012) Synthesis, characterization, and antimicrobial activity of zinc oxide nanoparticles against human pathogens. *BioNanoScience* 2:329–335. https://doi.org/10.1007/s12668-012-0061-6

43. Ahamed M, Alhadlaq HA, Khan MA, Karuppiah P, Al-Dhabi NA (2014) Synthesis, characterization, and antimicrobial activity of copper oxide nanoparticles. *J Nanomater* 2014. https://doi.org/10.1155/2014/637858

44. Ananth A, Dharaneedharan S, Heo M-S, Mok YS (2015) Copper oxide nanomaterials: Synthesis, characterization and structure-specific antibacterial performance. J *Chem Eng* 262:179–188. https://doi.org/10.1016/j.cej.2014.09.083

45. Klink MJ, Laloo N, Leudjo Taka A, Pakade VE, Monapathi ME, Modise JS (2022) Synthesis, Characterization and Antimicrobial Activity of Zinc Oxide Nanoparticles against Selected Waterborne Bacterial and Yeast Pathogens. Molecules 27:3532. https://doi.org/10.3390/molecules27113532

46. Yang H, Ze-Sheng L, Qian H, Yang Y, Zhang X, Sun C (2004) Molecular dynamics simulation studies of binary blend miscibility of poly (3-hydroxybutyrate) and poly (ethylene oxide). Polym 45:453–457. https://doi.org/10.1016/j.polymer.2003.11.021

47. Ryjkina E, Kuhn H, Rehage H, Müller F, Peggau J (2002) Molecular Dynamic Computer Simulations of Phase Behavior of Non-Ionic Surfactants. *Angew Chem Int Ed* 41:983–986. https://doi.org/10.1002/1521-3773

48. Fan CF, Olafson BD, Blanco M, Hsu SL (1992) Application of molecular simulation to derive phase diagrams of binary mixtures. Macromolecules 25:3667–3676. https://doi.org/10.1021/ma00040a010

49. Campos A, Gómez CM, García R, Figueruelo JE, Soria V (1996) Extension of the Flory-Huggins theory to study incompatible polymer blends in solution from phase separation data. Polym 37:3361–3372. https://doi.org/10.1016/0032-3861(96)88483-7

50. Knetsch MLW, Koole LH (2011) New Strategies in the Development of Antimicrobial Coatings: The Example of Increasing Usage of Silver and Silver Nanoparticles. Polym 3:340–366. https://doi.org/10.3390/polym3010340

51. Busscher HJ, Uyen MH, Van Pelt AW, Weerkamp AH, Arends J (1986) Kinetics of adhesion of the oral bacterium Streptococcus sanguis CH3 to polymers with different surface free energies. *Appl Environ Microbiol* 51:910–914. https://doi.org/10.1128/aem.51.5.910-914.1986

52. Katsikogianni M, Spiliopoulou I, Dowling DP, Missirlis YF (2006) Adhesion of slime producing Staphylococcus epidermidis strains to PVC and diamond-like carbon/silver/fluorinated coatings. *J Mater Sci: Mater Med* 17:679–689. https://doi.org/10.1007/s10856-006-9678-8

53. Almaguer-Flores A, Ximénez-Fyvie LA, Rodil SE (2010) Oral bacterial adhesion on amorphous carbon and titanium films: effect of surface roughness and culture media. Journal of Biomedical Materials Research Part B: Applied Biomaterials: An Official Journal of The Society for Biomaterials, The Japanese Society for Biomaterials, and The Australian Society for Biomaterials and the Korean Society for Biomaterials 92:196–204. https://doi.org/10.1002/jbm.b.31506

54. Pavithra D, Doble M (2008) Biofilm formation, bacterial adhesion and host response on polymeric implants—issues and prevention. *Biomed Mater* 3:034003. https://doi.org/10.1088/1748-6041/3/3/034003

55. Liu Y, He L, Mustapha A, Li H, Hu ZQ, Lin M (2009) Antibacterial activities of zinc oxide nanoparticles against Escherichia coli O157: H7. *J Appl Microbiol* 107:1193–1201. https://doi.org/10.1111/j.1365-2672.2009.04303.x

56. Ayawei N, Ekubo AT, Wankasi D, Dikio ED (2015) Adsorption of congo red by Ni/Al-CO3: equilibrium, thermodynamic and kinetic studies. *Orient J Chem* 31:1307. https://doi.org/10.13005/ojc/310307

57. Ayawei N, Ebelegi AN, Wankasi D (2017) Modelling and Interpretation of Adsorption Isotherms. *J Chem* 2017:1–11. https://doi.org/10.1155/2017/3039817

58. Piccin JS, Dotto GL, Pinto LAA (2011) Adsorption isotherms and thermochemical data of FD&C Red n 40 binding by chitosan. *Braz J Chem Eng* 28:295–304. https://doi.org/10.1590/S0104-66322011000200014